Polarized Response of East Asian Winter Temperature Extremes in the Era of Arctic Warming

SHUANGMEI MA, CONGWEN ZHU, AND BOQI LIU

State Key Laboratory of Severe Weather, and Institute of Climate System, Chinese Academy of Meteorological Sciences, Beijing, China

TIANJUN ZHOU

LASG, Institute of Atmospheric Physics, Chinese Academy of Sciences, Beijing, China

YIHUI DING

National Climate Center, China Meteorological Administration, Beijing, China

YVAN J. ORSOLINI

Norwegian Institute for Air Research (NILU), Kjeller, Norway

(Manuscript received 12 July 2017, in final form 4 April 2018)

ABSTRACT

It has been argued that fewer cold extremes will be expected to occur over most midlatitude areas, because of anthropogenic-induced global warming. However, East Asia repeatedly suffered from unexpected cold spells during the winter of 2015/16, and the low surface air temperature (SAT) during 21–25 January 2016 broke the previous calendar record from 1961. We hypothesize that cold extremes such as these occur because of Arctic amplification (AA) of global warming. To test this hypothesis, we analyzed the changes of SAT variability in the winter season over East Asia. Our results show that the SAT variability (measured by the standard deviation of the winter season daily mean SAT) over East Asia has significantly increased in the era of AA during 1988/89–2015/16 and exhibits a polarization between warm and cold extremes, popularly dubbed as ''weather whiplash.'' This phenomenon is driven by both the thermodynamic effects of global warming and the dynamic effects of AA. Global warming favors a rising SAT and more frequent warm extremes. The AA phenomenon strengthens the wavy components of midlatitude circulation, leading to more frequent blockings over the Ural region and a stronger Siberian high in north Asia. This dynamic effect of AA enhances the intrusion of cold air from Siberia into East Asia and causes cold extremes. Because there is a comparable increase of frequency of both warm and cold extremes, the SAT variability significantly increases in unison with AA, but little change is observed in the seasonal mean SAT of East Asia. This implies increased risks of both cold and warm extremes over East Asia exist even during global warming.

1. Introduction

Wintertime blockings over the Urals thermally enhance cold advection downstream (Cheung et al. 2012) and are usually accompanied by an amplification of the cold surface Siberian high (SH) (Takaya and Nakamura 2005) and subsequent cold-air outbreaks into East Asia (Park et al. 2014; Yang et al. 2018). Frequent blocking over the Urals together with amplified SH has been considered the most characteristic weather circulation of a stronger East Asian winter monsoon (EAWM) (Nakamura et al. 2016). Persistent blocking over the Urals and an intensified SH favor the southward intrusion of cold air via persistent cold-air advection downstream and surface northerly flows, thus dominating the local winter weather and climate over East Asia (Zhang et al. 1997; Wang et al. 2010; Park et al. 2014; Nakamura et al. 2016). The rapid Arctic warming could have enhanced the SH and the occurrence of blocking events over the Urals and further contributed to the frequent Eurasian cold winters and extreme cold spells of the past decades (Honda et al. 2009; Cohen et al. 2012;

Corresponding author: Congwen Zhu, zhucw@cma.gov.cn

DOI: 10.1175/JCLI-D-17-0463.1

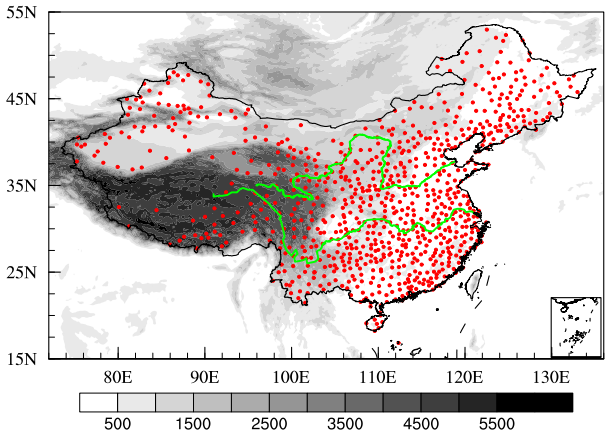

FIG. 1. The spatial distribution of the 839 observation stations used in this study. The shaded area indicates the terrain height (m). The bottom-right corner shows the map of the South China Sea.

Francis and Vavrus 2012; Liu et al. 2012; Zhang et al. 2012; Tang et al. 2013; Mori et al. 2014; Luo et al. 2017; Yao et al. 2017). Although many studies have argued for links between Arctic amplification (AA) and mid-latitude weather or climate and their extremes, this issue remains poorly understood and is still debated (Cohen et al. 2014; Barnes et al. 2014; Wallace et al. 2014; Shepherd 2016; Overland et al. 2016; Screen 2017).

The variation in the EAWM is closely related to the El Niño–Southern Oscillation (ENSO) phenomena. The EAWM is generally weaker with higher surface air temperature (SAT) during strong El Niño events, and the stronger EAWM usually corresponds to cold SAT over East Asia during strong La Niña events (Zhang et al. 1997; Cheung et al. 2012; Ding et al. 2014). The global mean SAT during the boreal winter season (November–March) of 2015/16 reached a record high, accompanied by the strongest El Niño episode on record (Zhai et al. 2016). Based on the records of meteorological stations (Fig. 1), an above-normal winter mean SAT was observed in China (Fig. 2a). However, eastern China was repeatedly subject to severe cold events during this cold season, and the most severe cold surge caused the SAT to drop sharply around 21–25 January (Fig. 2b). This extreme cold corresponded with a minimum of the daily minimum SATs of −10°C, which occurred in most areas of China, allowing the 0°C isotherm of the daily minimum SATs to reach south China (Fig. 2c). In contrast to the corresponding periods over the past three decades, the largest cold SAT anomalies occurred in north China, with more than −5°C anomalies spanning eastern China (Fig. 2d). The average SAT over eastern China during 21–25 January 2016 was −7.5°C, which is 5.2°C colder than normal, breaking the calendar record of extreme cold since at least 1961 (Fig. 2e). The record-low minimum SATs in January were observed at many weather stations (8% stations), and most of the station-observed SATs passed the extreme cold threshold (92% stations). This resulted in a considerable power load increase as well as a greater number of patients in hospitals, more widespread disruption to transportation, and considerable damage to agricultural crops [China Meteorological Administration (CMA) 2017]. This extraordinary cold surge even swept southward to Thailand and caused the deaths of 14 people (CMA 2016).

It is evident that the variability of daily SATs became larger across the cold and warm extremes during the cold season of 2015/16, concurrently with more frequent colder and warmer extremes (Fig. 2f), and exhibited a polarization over East Asia during this winter under the warmest global SAT with the influence of a super El Niño (i.e., an unusually strong El Niño). Such a polarization is popularly referred to as "weather whiplash." The large variability of daily SAT caused the public to raise the question: How can more frequent warm extremes coexist with increased occurrences of damaging and life-threatening cold extremes under global warming? In fact, a similar and unexpected cold extreme with heavy snowfall also occurred in North America in early January 2014, which has already led to increased concern and debate among atmospheric scientists (Wallace et al. 2014; Van Oldenborgh et al. 2015; Screen et al. 2015). The temperature of the source region of cold air is argued to be the dominant factor in determining cold temperature extremes. Thus, fewer cold events and lower SAT variability in the northern mid–high latitudes are expected as a thermodynamic response to AA (Screen 2014; Screen et al. 2015; Sun et al. 2016; Van Oldenborgh et al. 2015).

It is suggested that both dynamic (changes in the large-scale atmospheric circulations) and thermodynamic (rising temperatures resulting from global warming) climate influences have contributed to the changes of temperature extremes over the past 35 years (Horton et al. 2015; Shepherd 2016; Overland et al. 2016; Screen 2017). Global warming is thermodynamically expected to increase (decrease) the frequency and intensity of extreme hot (cold) events (IPCC 2012; Fischer and Knutti 2015) and to substantially contribute to the observed more (less) frequent hot (cold) extremes and the observed decrease in temperature variability in northern high-latitude continents and North America (Screen 2014; Screen et al. 2015; Sun et al. 2016; Van Oldenborgh et al. 2015; Horton et al. 2015). Nevertheless, the risk of extreme temperatures over some regions has also been altered by recent changes in the regional circulation resulting from

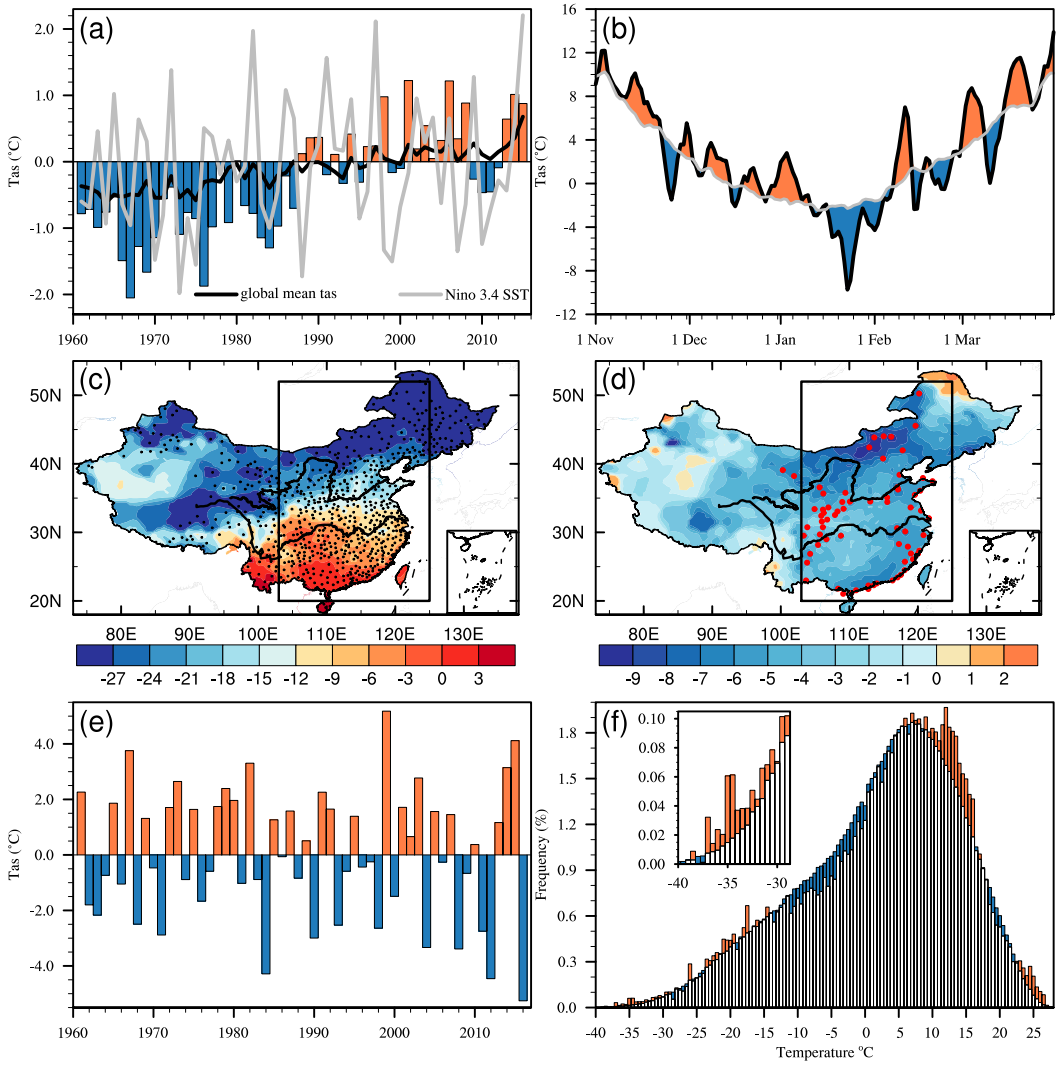

FIG. 2. (a) Time series of the November–March mean temperatures averaged over continental China (color bars), the global mean temperature (black line), and the Niño-3.4 index (gray line) during 1961–2016. (b) Daily mean SATs averaged over eastern China [EC; i.e., the black rectangular box bounded by 20°–52°N, 103°–125°E in (c) and (d)] during 1 Nov 2015–31 Mar 2016 (colored shading and thick black line) and the daily climatology (gray line). (c) Minimum (shading) of the daily minimum SATs (Tmin) during January 2016. Stations where the minimum daily Tmin in January 2016 was less than or equal to the threshold of extreme low temperatures, which is defined as temperatures below the 10th percentile of the daily Tmin of January during the reference periods, are shown with black dots. (d) The daily mean temperature anomalies (shading; °C) for the cold spell during 21–25 Jan 2016. The stations for which the minimum of the daily Tmins in January 2016 were below the observed records are plotted as red dots. (e) The time series for the 21–25 Jan daily mean temperature anomalies averaged over EC during 1961–2016. (f) Histogram of the cold-season daily mean temperatures averaged over EC. The orange bars are for 2015/16 and the blue bars are for the mean of the reference period 1979/80–2015/16. The global mean SATs in (a) are derived from GISTEMP.

spatially nonuniform warming, especially with respect to AA (Overland et al. 2016; Francis and Vavrus 2012; Cohen et al. 2014; Honda et al. 2009; Liu et al. 2012; Zhang et al. 2012; Tang et al. 2013; Mori et al. 2014; Horton et al. 2015; Yao et al. 2017; Luo et al. 2017). The polarization of East Asian SATs (i.e., intensified weather whiplash) during the cold season of 2015/16 led us to investigate the existence of substantial changes of SAT variability over East Asia and try to explore whether climate change can thermodynamically and dynamically contribute to the observed changes of extreme temperatures over East Asia.

In this study, we will emphasize SAT variability during the cold season over East Asia instead of cold-season

mean SAT. The goal of this study is to analyze the long-term change in SAT variability over East Asia in the era of AA (1988/89–2015/16; Cohen et al. 2014) and attempt to answer whether there is a significantly intensified trend of weather whiplash. Of particular interest is to understand the dynamic and thermodynamic characteristics of changes in weather whiplash over East Asia in response to AA. We find the East Asian SAT variance significantly increased in the era of AA (i.e., it exhibits an intensified tendency of weather whiplash). We show evidence that the increase in SAT variability is due to both dynamic and thermodynamic effects of global warming, with general global warming thermodynamically contributing to more warm extremes while the dynamical impacts of AA contribute to more cold extremes.

2. Data and methods

a. Data description

The observed daily minimum, maximum, and mean SATs of 839 stations with continuous records throughout the period of 1961–2016 from the China National Meteorological Information Center (NMIC; http://data.cma.cn/en) are used. This dataset is subject to quality control, including extreme value control, consistency check, and correction of suspected and erroneous data, before the NMIC releases it (Liu and Ren 2005). It is considered the best daily dataset used for the climate study of China (Sun et al. 2014). The distribution of meteorological stations used in this study is shown in Fig. 1. To calculate the area-weighted mean, the station statistics of the SAT measurements are interpolated onto a 0.5° × 0.5° resolution grid using an iterative improvement objective analysis with a search radius of 3°–2°–1°–0.5° with the ''obj_anal_ic_Wrap'' function in the NCAR Command Language (http://www.ncl.ucar.edu/Document/Functions/Contributed/obj_anal_ic_Wrap.shtml). For example, to estimate the East Asia area-averaged histogram of daily mean SATs shown in Fig. 2f, the daily mean SATs at each station in each winter were divided into intensity bins of 0.5°C, and the frequencies of each intensity bin were calculated. Then, the station SAT frequencies of each intensity bin were interpolated onto a 0.5° × 0.5° grid. Finally, these 0.5° grid cells were averaged using the area as the weight to calculate the regional averages for each intensity bin.

Monthly SAT values from the Goddard Institute for Space Studies Surface Temperature Analysis (GISTEMP; Hansen et al. 2010, http://data.giss.nasa.gov/gistemp) and atmospheric circulation data obtained from the ERA-Interim reanalysis (Dee et al. 2011, http://apps.ecmwf.int/datasets) are also used. Distributions of the seasonal mean SAT on a global scale and SAT variabilities over China are estimated from the ERA-Interim and NMIC data, respectively, unless otherwise specified. The Niño-3.4 index and Arctic Oscillation (AO) index are obtained from the NOAA Climate Prediction Center website (https://www.esrl.noaa.gov/psd/data/climateindices/list/).

b. Methods

1) Statistical analysis

Following Cohen (2016) and Sun et al. (2016), we measured the SAT variability during the winter season by the standard deviation of the daily mean SAT at each grid or station during the winter season in each year. Then, we estimated the intra-annual time series of the averaged daily SAT variability over East Asia. Because we applied the yearly varied mean of daily SAT for each winter season to normalize the daily SAT time series, this to a great extent avoided the linear trend of mean SAT spuriously increasing the variance.

The least squares linear regression method is used to estimate the linear trends of climate variables. Following previous studies (Cohen et al. 2014; Cohen 2016), the trends are calculated based on the EAWM seasonal (November–January) mean values during the period 1988/89–2015/16, which matches the full period of the AA era (Cohen et al. 2014). The climatological mean and correlation are calculated during the period 1979/80–2015/16, and the daily climatology is defined as the 37-yr daily mean during the same time period. The statistical significances of the trends and correlation coefficients are calculated using a two-tailed Student's t test.

The daily temperature and horizontal winds at 850 hPa are first derived from the 6-hourly data of the ERA-Interim reanalysis and are then used to calculate temperature advection. Finally, the seasonal mean of the cold advection of temperature is obtained by masking the warm advection {i.e., the seasonal mean of the cold advection of temperature is the mean of temperature advection of days with daily temperature advection $-[u(\partial T/\partial x) + v(\partial T/\partial y)] < 0$}. Similarly, the seasonal mean 850-hPa horizontal wind associated with cold advection is defined as the mean of 850-hPa horizontal wind of days with daily temperature advection $-[u(\partial T/\partial x) + v(\partial T/\partial y)] < 0$.

2) Wave activity flux

The wave activity flux (WAF) for stationary Rossby waves introduced by Takaya and Nakamura (2001) is adopted to diagnose the propagation of wave activity

associated with AA. The horizontal components of stationary WAF in pressure coordinates are derived as

$$\mathbf{W} = \frac{1}{2|\overline{\mathbf{u}}|}\begin{Bmatrix} \overline{u}(\psi_x'^2 - \psi'\psi'_{xx}) + \overline{v}(\psi'_x\psi'_y - \psi'\psi'_{xy}) \\ \overline{u}(\psi'_x\psi'_y - \psi'\psi'_{xy}) + \overline{v}(\psi_y'^2 - \psi'\psi'_{yy}) \end{Bmatrix}. \quad (1)$$

In Eq. (1), the overbars and primes denote the climatology and its deviation, respectively; the subscripts x and y represent the zonal and meridional gradients, respectively; ψ is the streamfunction; and $|\overline{\mathbf{u}}|$ is the magnitude of the climatological wind.

3) MEANDERING AND BLOCKING INDEX

To measure the waviness of the midtroposphere, the meandering index is calculated over the Eurasian sector (0°–90°N, 0°–180°) using the monthly geopotential height at 500 hPa (Z500) from the ERA-Interim reanalysis. Following Di Capua and Coumou (2016), the meandering index is defined as the maximum waviness in geopotential height contours at any given season, using all information of the full spatial position of each contour. Same as the previous studies (Liu et al. 2012; Tang et al. 2013), blocking events are defined as the intervals when the daily Z500 anomalies are higher than one standard deviation away from the cold-season climatological mean for each grid cell during five consecutive days. Meanwhile, the area mean of blocking events over the Ural region, bounded by 50°–80°N and 40°–90°E, is calculated.

4) COLD AND WARM EXTREMES

Extremely cold (warm) days are defined as days with daily minimum (maximum) SATs lower (higher) than the 10th (90th) percentile of the daily minimum (maximum) SAT during the cold season for the period 1979/80–2015/16.

3. Results

a. Changes of SAT variability over East Asia

Inspired by the polarization of East Asian SATs during winter of 2015/16, we investigate the existence of substantial changes of SAT variability over East Asia. To answer this question, we calculated the standard deviation of the daily mean SAT in the EAWM season to measure the variability of SAT (also referred to as the SAT difference between warmer and colder days). Figure 3 shows the linear trends of the daily SAT variability over China and the time series of SAT variability averaged over eastern China in the EAWM seasons of 1988/89–2015/16. The daily SAT variability during the EAWM season increases significantly across China, aside from the Tibetan Plateau. The eastern China area-averaged standard deviation of the daily mean SATs increased at a rate of 0.26°C decade^{-1}, which is statistically significant at the 99% confidence level (two-tailed Student's t test). The long-term tendency of the enhanced daily SAT variability over East Asia during the cold season can be captured well by the ERA-Interim reanalysis (Fig. 4), which shows a spatial correlation of +0.86 to observational data over China, with an even higher temporal correlation with the time series of SAT variability in East Asia ($r = 0.99$). A significant decline in the daily SAT variability can be observed over the northern high latitudes in Canada and in central to eastern North America from the ERA-Interim reanalysis results, which is consistent with the results of Screen (2014) and Screen et al. (2015) and implies a possible impact of AA by a thermodynamic effect owing to advection of warmer air masses (Screen 2014; Screen et al. 2015; Screen 2017; Van Oldenborgh et al. 2015; Sun et al. 2016; Rhines et al. 2017). Meanwhile, it can be seen that the increase in variability across Asia and the decrease in variability over the North American high-latitude region dominate the zonal mean signal across the continents, and thus is consistent with the result of Cohen (2016), who found a decrease in the temperature variability across the high latitudes but an increase in the midlatitude continents.

b. Correlation between East Asia SAT variability and Arctic warming

A recent study suggests the impacts of Arctic warming on local climates are different in North America and East Asia (Kug et al. 2015), where regional extreme temperatures are largely influenced by AA-induced regional circulation patterns (Horton et al. 2015). To determine whether the increased SAT variability in the winter season is correlated with Arctic warming, we examined the correlation coefficients of the East Asian area-averaged SAT variability and the seasonal mean SAT anomalies over the Northern Hemisphere. Significantly positive correlations are evident over the Arctic, with higher r values than those with detrending (Figs. 5a,b). In addition, EAWM-season SAT variability regressed on the standardized Arctic SAT exhibits significantly positive values in eastern China; the same is true for nearly all of China, except for the Tibetan Plateau (Figs. 5c,d), which is consistent with the long-term tendencies in SAT variability (Fig. 3a).

c. The mechanistic connection between AA and changes in East Asia SAT variability

Notably, AA corresponds to a stronger surface warming over the Arctic relative to the rest of the Northern

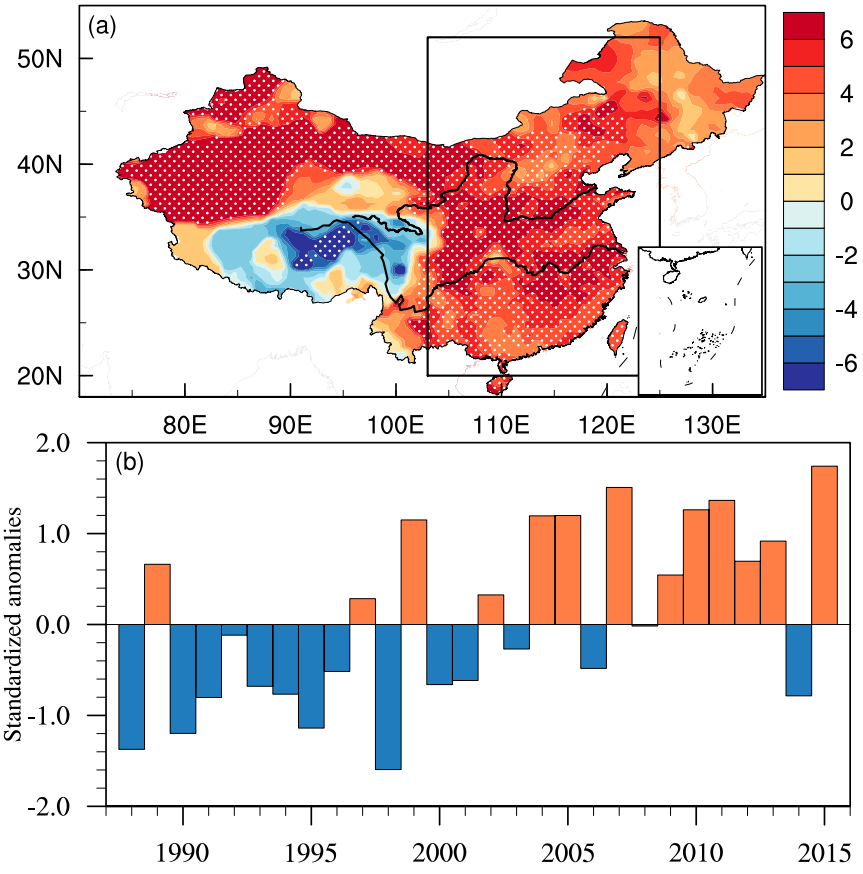

FIG. 3. (a) Linear trends (% decade^{-1}; shading; dots represent significance at the 95% level) of the SAT variability in the cold season (November–March) for the period 1988/89–2015/16. Trends are normalized by their climatological means. (b) Time series of the standardized anomalies of the cold-season SAT variabilities averaged over eastern China [as indicated by the box in (a)]. Data are taken from NMIC.

Hemisphere with a strong cooling center over Siberia (Fig. 6a), the "warm Arctic, cold continents" phenomenon. This is related to the Arctic change and has been regarded as the main driver of the reduced meridional temperature gradient (Inoue et al. 2012; Cohen et al. 2014; Sun et al. 2016). Consequently, the zonal winds over Eurasia are theoretically weakened owing to the physical constraints of the thermal wind adjustment, which is confirmed by the negative trend of westerlies in the tropospheric midlatitudes (Fig. 6b), where the weakened zonal westerly wind itself tends to enhance a wavier meandering flow pattern. The slowdown of the eastward propagation of Rossby waves induced by the weakened westerlies (according to the relationship between the Rossby phase speed and mean westerly wind speed $c = \overline{U} - \beta/k^2$) can also further enhance a broader meander. The meandering index, which is defined to measure the waviness of the midtroposphere over Eurasia, shows a significant upward trend under the background of AA (Fig. 6d). Consequently, blocking events over the Urals (50°–80°N, 40°–90°E) are favored (Fig. 7c), consistent with previous results (Luo et al. 2017; Yao et al. 2017).

Meanwhile, AA corresponds to an upper-troposphere wave train across the Eurasian continent, which is characterized by a significant tendency toward ridge–trough–ridge patterns in the time evolution of the geopotential height at 250 hPa (Z250), with the southeastward propagation of WAF (Fig. 6c). Such a result is consistent with previous studies (Hoskins and Ambrizzi 1993; Honda et al. 2009; Inoue et al. 2012), which also suggest that this stationary Rossby wave is generated by anomalous turbulent heat (low-level diabatic heating through the sensible and latent heat flux) as a result of anomalous ice cover over the Barents–Kara Sea. The enhanced ridge over the Ural region (50°–80°N, 40°–90°E) is favorable for the formation and maintenance of blockings. The anomalous upper-level anticyclone enhances the anomalous surface easterlies and gives rise to colder air piling up near Lake Baikal (Honda et al. 2009). In the meantime, the weakened tropospheric

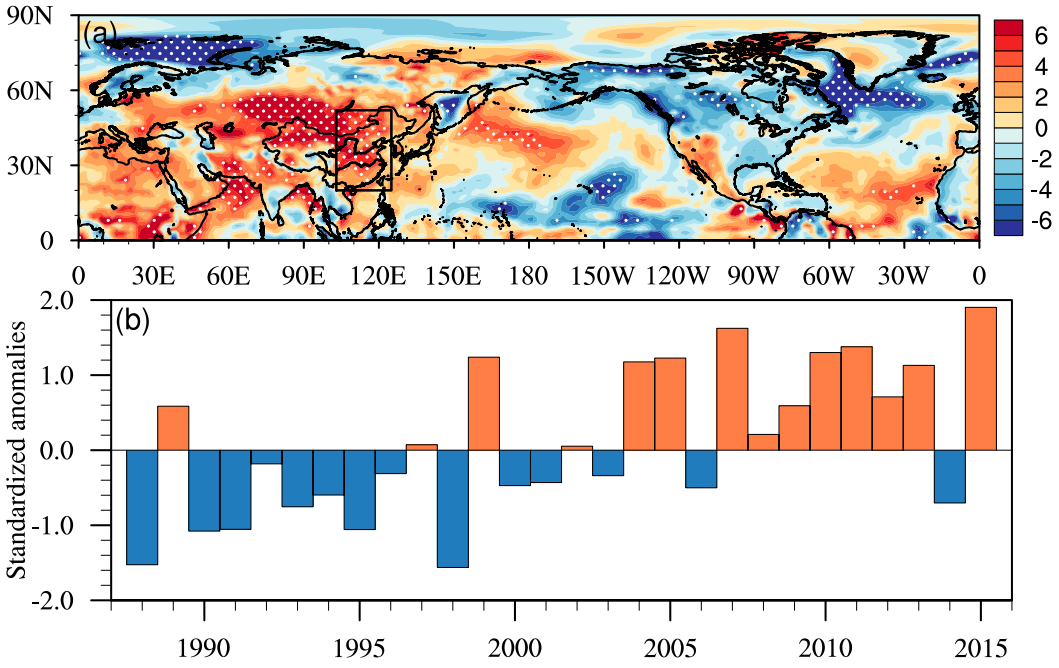

FIG. 4. (a) Linear trends (% decade^{-1}; shading; dots represent significance at the 95% level) of SAT variability during the cold season (November–March) for the period 1988/89–2015/16. The trends are normalized by their climatological means. (b) The time series of the standardized anomalies of the cold-season SAT variabilities averaged over eastern China [as indicated by the box in (a)]. Data are taken from the ERA-Interim reanalysis.

westerlies of the midlatitudes reduce the eastward movement of the cyclone-related moist and warm air from the North Atlantic Ocean (Zhang et al. 2012; Honda et al. 2009; Inoue et al. 2012). Consequently, these two physical processes enhance the SH (Fig. 7e). In addition, the increase of local snow cover results in stronger diabatic cooling and further enhances the SH, affecting the anticyclonic circulation and promoting Arctic warming (Cohen et al. 2012; Orsolini et al. 2013). Hence, the Eurasian snow anomalies by themselves could further reinforce the warm arctic, cold continents pattern.

Such cold-type circulation anomalies with more blocking events over the Urals and an amplified SH may cause cold Arctic air to migrate southward into East Asia (Francis and Vavrus 2012; Liu et al. 2012; Mori et al. 2014), leading to the severe cold extremes there and enhancing the SAT variability over East Asia. This dynamic effect of AA on East Asian climates is supported by the results of several studies (Zhang et al. 2012; Tang et al. 2013; Barnes et al. 2014; Di Capua and Coumou 2016; Luo et al. 2017; Yao et al. 2017), and the Arctic sea ice loss associated with AA has been regarded as the main driver of the dynamic effect of AA (Honda et al. 2009; Cohen et al. 2012; Liu et al. 2012; Mori et al. 2014). Some model simulations driven by Arctic sea ice loss have revealed that the response of the atmospheric circulation over Eurasia favors more frequent cold extremes and the increase of SAT variability over East Asia (Screen 2014; Screen et al. 2015). In addition, high-resolution coupled ocean–atmosphere simulations of the 2007 extreme sea ice reduction show that the largest effect on winter SAT occurs along the Pacific coast of East Asia and over eastern China in particular (Orsolini et al. 2012), leading to cold anomalies. Thus, it is evident that the increase in the SAT variability over East Asia is closely linked to AA. The AA contributed to more cold extremes over East Asia through facilitating more blocking events over the Ural region and a strengthened SH.

The regressions of Z250 and the associated WAF, atmospheric blocks, and sea level pressures (SLPs) with the average SAT variability of East Asia show broadly similar patterns over the Eurasian continent relative to those with the Arctic SAT anomalies; namely, a wave train propagating southeastward that is significantly related to the increased blocking events over the Urals and strengthened SH (Fig. 7). With respect to the rapid Arctic warming, the trend of the mean Z250 depicts a significantly deepened ridge–trough pattern, with an intensified southeastward propagation of WAF during the AA era of 1988/89–2015/16 (Fig. 6c); a significant positive trend in the blocking incidence appears over the Urals during the same period (Fig. 8a). Moreover, SLP exhibits a significant increasing trend over Siberia,

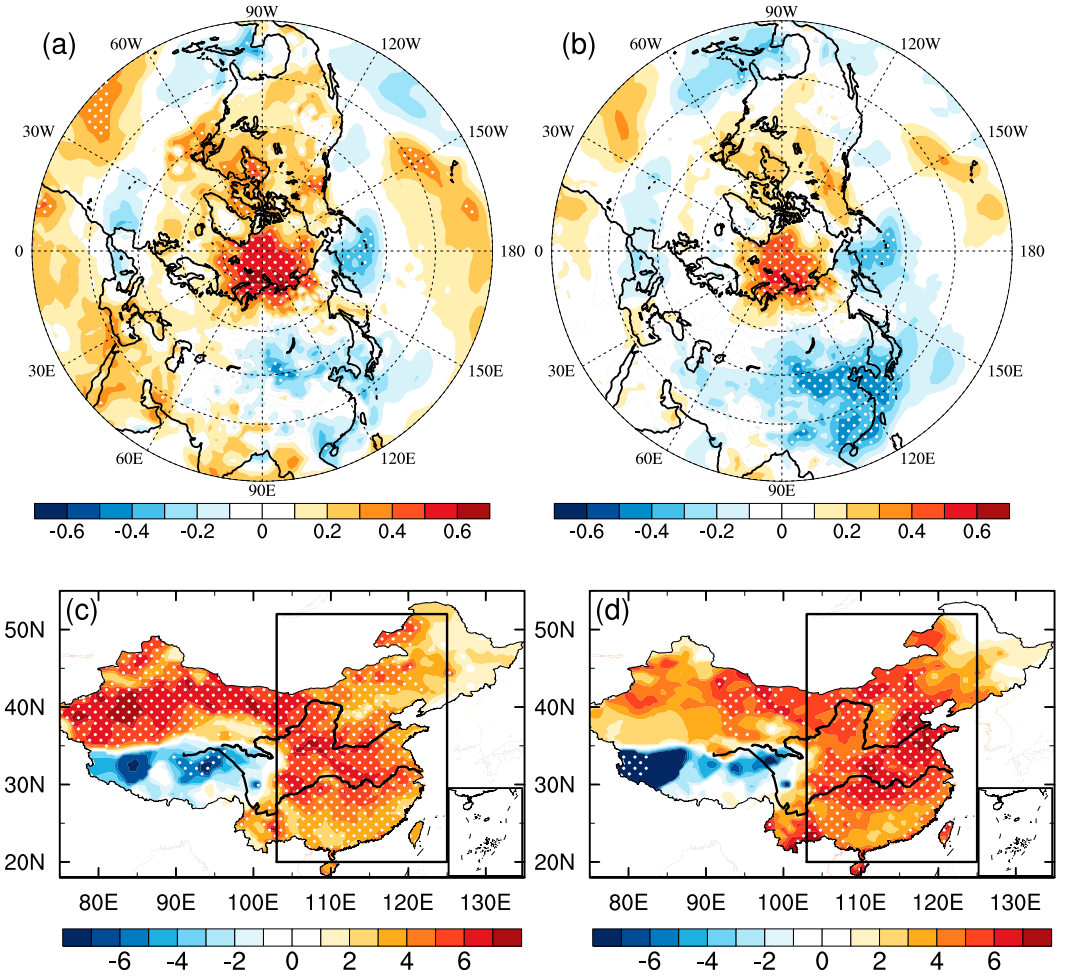

FIG. 5. Relationships between the Arctic air temperature and cold-season variability of the daily SATs over China during 1979/80–2015/16. (a) Correlation coefficients between SAT and SAT variability anomalies averaged over eastern China [the rectangular box in (c) and (d)]. (b) As in (a), but for the detrended anomalies. (c) Linear regression (% $°C^{-1}$) of the normalized SAT variability (divided by the climatological mean) over China on the Arctic SAT (averaged over 60°–90°N, 0°–360°E). (d) As in (c), but for the detrended anomalies. Stippling indicates significance at the 95% level.

accompanied by an enhanced northeasterly flow on the southwest flank of the SH (Fig. 8b). The stronger northerlies over eastern Siberia tend to cause stronger cold advection bringing cold air from northeastern Siberia to the downstream East Asian region. Coinciding with the strengthening trend of the Eurasia cold high, a significantly intensified cold-air advection at 850 hPa is observed over East Asia (Fig. 8c). In addition, along with an exceptional upward trend of SH intensity and the frequency of blocking events averaged over the Urals, the intensity of East Asian cold advection exhibits an obvious intensifying trend (Fig. 8d). Therefore, this evidence confirms that rapid Arctic warming is significantly related to the increased cold extremes over East Asia through the dynamic impacts of AA and then contributes to the increased SAT variability.

The thermodynamic effects of human-induced global warming favor warm extremes (IPCC 2012; Wallace et al. 2014; Shepherd 2016), dramatically increasing their frequency (Fischer and Knutti 2015; Sun et al. 2014; Christidis et al. 2015). The correlation coefficient r between the detrended global average SAT and East Asian mean frequency of warm extremes is 0.41, which is statistically significant at the 0.01 level, and r increases to 0.7 when linear trends in both time series are not removed. Along with the significantly warming trend of winter global mean SAT, the warm extremes over East Asia show an obvious increasing trend (Fig. 9). The significant correlation between global mean SAT and East Asian warm extremes and the coincidence of an increasing trend of warm extreme events with global warming indicate that global warming thermodynamically increases warm

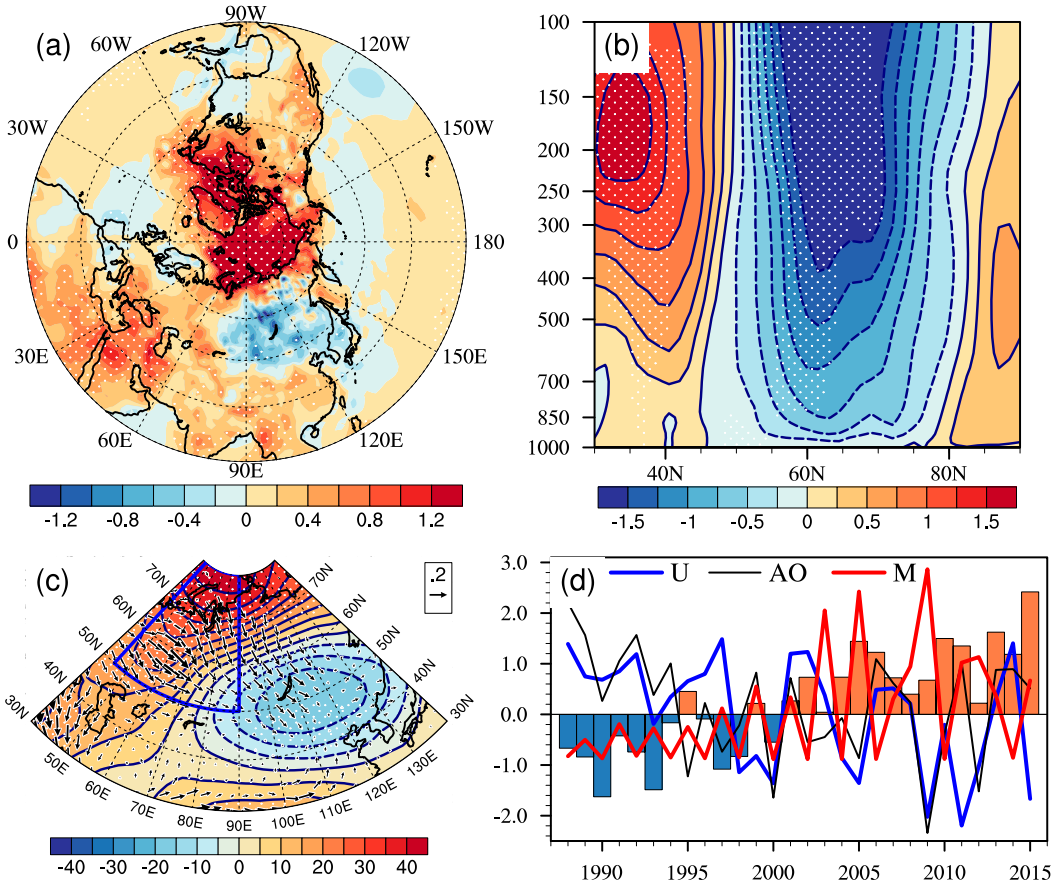

FIG. 6. (a) Linear trends of the cold-season mean SAT (shading; °C decade^{-1}) during the period 1988/89–2015/16. (b) Linear trends in the zonal mean zonal wind over the vertical cross section (shading and contours; zonally averaged over 70°–120°E; m s^{-1} decade^{-1}). (c) Trends of geopotential height at 250 hPa (shading and contours; m decade^{-1}; superimposed vectors show the 250-hPa horizontal components of the WAF trends). Stippling in (a)–(c) indicates significance at the 95% confidence. The blue box in (c) indicates the Ural region. (d) The standardized time series of the seasonal mean Arctic SAT averaged over 60°–90°N, 0°–360°E (bars), zonal wind at 500-hPa averaged over the region of 50°–70°N, 70°–120°E (*U*, blue line), AO index (thin black line), and meandering index (*M*, red line).

extreme events over East Asia and then promotes the increase of SAT variability. Therefore, we conjecture that the increased SAT variability over East Asia is caused by both the thermodynamic effects of global warming through increasing warm extremes and the dynamic effects of AA through increasing cold extremes.

The observed increase of East Asian SAT variability is consistent with the model-projected response to continued Arctic sea ice loss and amplification of warming, which exhibit weak cooling, patches of increased standard deviation, and slightly increased probabilities of cold extremes in eastern Asia (i.e., China, Mongolia) (Screen et al. 2015). This provides another line of evidence that AA may have contributed significantly to the polarization of the daily SATs over East Asia. The winter climate anomalies in East Asia are closely linked to the internal atmosphere fluctuations associated with ENSO and the AO (Ding et al. 2014; Zhai et al. 2016); however, the East Asian SAT variability is not correlated with ENSO ($r = -0.08$) and AO ($r = -0.09$). The AO has been distinguished from the AA (Liu et al. 2012; Mori et al. 2014), which is weakly correlated with the Arctic mean SAT ($r = 0.11$).

During the AA era of 1988/89–2015/16 (Cohen 2016), the cold-season Arctic SAT averaged over 60°–90°N, 0°–360°E exhibited a warming trend of 0.99°C decade^{-1} with a loss of −11.75% decade^{-1} for sea ice concentration averaged over the Barents–Kara Sea (65°–85°N, 30°–90°E). The 500-hPa zonal wind averaged over Asia (50°–70°N, 70°–120°E) shows a weakening trend of −0.95 m s^{-1} decade^{-1}, with an increasing trend of 19.81% decade^{-1} for the meandering index defined over the Eurasian sector. Similarly, increasing trends of 0.82 hPa decade^{-1} are found for the intensity of SH,

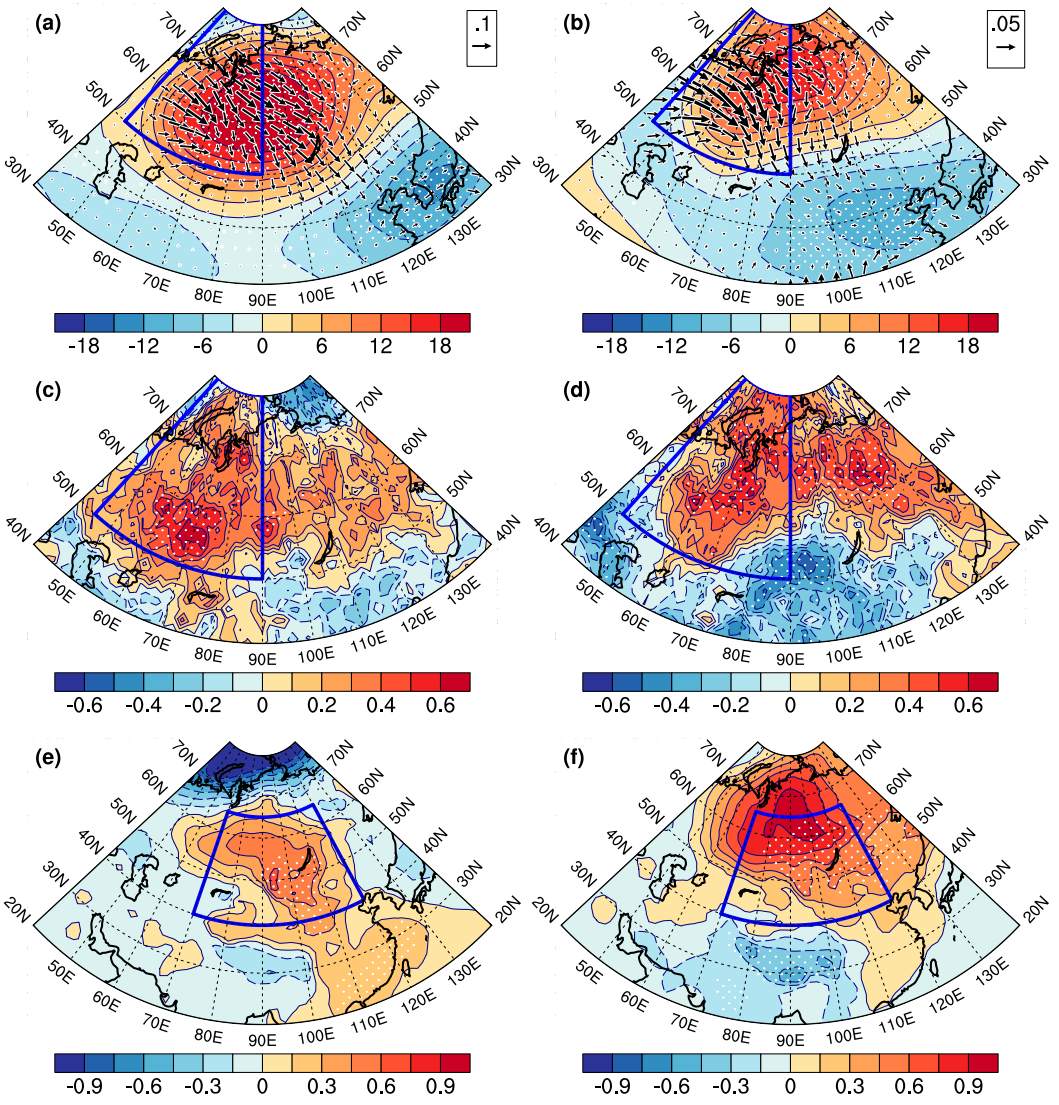

FIG. 7. Linear regression of the cold-season mean (a) 250-hPa geopotential height anomaly fields (m), (c) incidence of blocking events (counts), and (e) SLP (hPa) on the detrended standardized time series of the area-averaged Arctic SAT during 1979/80–2015/16. (b),(d),(f) As in (a),(c),(e), but for regressing on the detrended standardized time series of SAT variability averaged over eastern China (20°–52°N, 103°–125°E). The superimposed vectors in (a) and (b) show the corresponding 250-hPa horizontal component of WAF ($m^2\,s^{-2}$). The white stippling denotes significant values at the 95% confidence level. The blue boxes in (a)–(d) and (e) and (f) indicate the Ural region and Siberian high domain, respectively. Data are taken from the ERA-Interim reanalysis.

25.50% decade^{-1} for the frequency of blocking events averaged over the Urals (50°–80°N, 45°–90°E), and 4.19% decade^{-1} for the cold advection of air temperatures at 850 hPa averaged over East Asia (20°–52°N, 103°–125°E). Although considerable interannual variabilities are superposed on these trends, the trends are significant at the 0.05 level (Fig. 10a). The standard deviation of the daily SAT averaged over East Asia increases by 4.93% decade^{-1}, which is significant at the 0.01 level. However, the cold-season mean SAT in this region exhibits a slightly insignificant warming. The histogram of the daily mean SAT distribution becomes wider over East Asia, implying that higher frequencies of colder and warmer extremes occurred during the warmer Arctic era (Fig. 10b). Hence, the frequencies of the cold and warm extremes exhibit significant increasing trends during the AA period, with rates of 13.08% and 11.39% decade^{-1}, respectively.

To further consolidate the linkage between AA and the SAT variability over East Asia, we examined the trend of Arctic mean SAT and East Asia area-averaged SAT variability, cold and warm extremes, as well as the

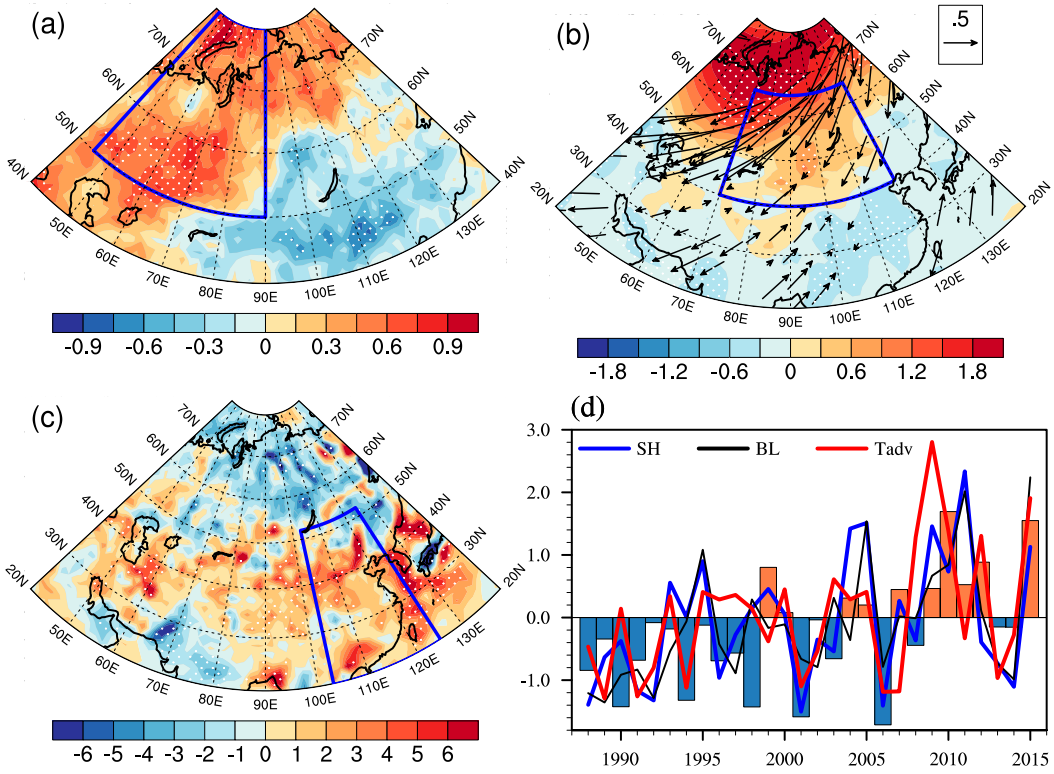

FIG. 8. Linear trend of the seasonal mean (a) frequency of blocking events (count decade^{-1}), (b) SLP (hPa decade^{-1}), and (c) cold advection of air temperature at 850 hPa (sign reversal; 10^{-6} K s^{-1} decade^{-1}) during the period 1988/89–2015/16. The vectors in (b) are the changes of the seasonal mean 850-hPa horizontal wind associated with cold advection. The white stippling in (a)–(c) indicates significance at the 95% confidence level. (d) Standardized time series of the frequency of cold extremes (bars) averaged over East Asia [20°–52°N, 103°–125°E, i.e., the box in (c)], seasonal mean SH (blue line) intensities, defined as the area-averaged SLP over the region of 40°–65°N, 70°–120°E [i.e., the box shown in (b)]; the blocking high events (BL; black line) averaged over the Urals [50°–80°N, 45°–90°E, as the box shown in (a)]; and the cold advection of temperature (Tadv; red line) averaged over East Asia during 1988/89–2015/16.

winter mean SAT during 1979/80–1997/98, when no prominent AA phenomenon was observed. During this time period, the Arctic SAT exhibited a weak warming linear trend or even slight cooling in some places, in contrast to the fastest warming of global-mean SAT anomaly (Kug et al. 2015; Yao et al. 2017). Specifically, the Arctic mean SAT exhibits a very weak warming trend of 0.01°C decade^{-1} during this period. Our results show that the extremely cold days averaged over East Asia decrease significantly at a rate of −48.50% decade^{-1}, but the extremely warm days increase significantly at a rate of 17.81% decade^{-1}. As a result, the average SAT variability over East Asia shows a significantly decreasing trend of −2.86% decade^{-1} and winter mean SAT shows a significantly warming trend of 0.11°C decade^{-1}.

The cold-season Arctic SAT anomalies were warmest in 2015/16 (Fig. 6d), whereas the zonal wind and meandering over Eurasia did not reach their extrema because of the impact of the positive phase of the AO. However, the weaker zonal wind, stronger meandering, and SH, in addition to more frequent blocking events over the Urals and anomalously strong cold-air advection over East Asia, have been observed in the Northern Hemisphere winter; these systems are linked to more cold extreme events and the maximum of SAT variability over eastern China (Figs. 5b, 6d, 8d). Thus, our hypothesized mechanisms are at play in the 2015/16 winter.

4. Summary and discussion

a. Summary

The polarization of East Asian daily SAT during the cold season of 2015/16 motivates the investigation in this study, which is whether there are substantial changes of SAT variability over East Asia, and whether climate change can thermodynamically and dynamically contribute to the observed changes of extreme temperature over

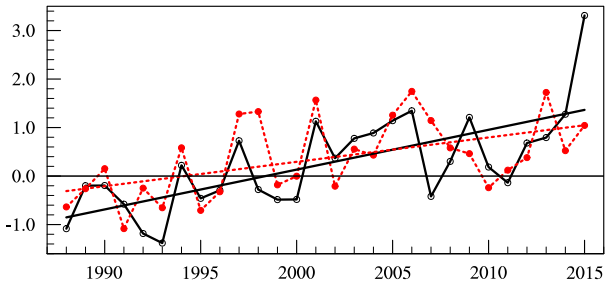

FIG. 9. The standardized time series of global average SAT (solid line with open circle) and frequency of warm extremes averaged over East Asia (dashed line with filled circle) and their linear trend during 1988/89–2015/16.

East Asia. Our results show that the SAT variability over East Asia has significantly increased by 4.93% decade^{-1} and exhibits polarization between warm and cold extremes in the era of AA.

The coactions of internal variability and the forced responses to climate change both affect extreme weather events (Cohen 2016; Shepherd 2016). Here, we conclude that the observed colder and warmer extremes over East Asia are a combined result of the dynamic effects of rapid Arctic warming and the thermodynamic effects of global warming. The rising SATs and more frequent warm extremes are thermodynamically favored by global warming. In contrast, the AA itself influences atmospheric circulation via making the midlatitude circulation wavier, with more frequent blockings over the Urals and a stronger Siberian high in north Asia. This dynamic effect of AA enhances the intrusion of cold air from Siberia into East Asia and causes the cold extremes. Hence, the SAT variability significantly increases in unison with Arctic warming, while little change is observed in the seasonal mean SAT over East Asia, because of the cancelling between these two effects.

The amplified SAT variability may exacerbate extreme conditions and result in a polarized response in the changes of SAT. Colder extremes with heavy snowfall and sleet are therefore more likely to be observed during the cold seasons in East Asia. Evidence suggests that climate warming has doubled the fatalities due to warm extremes and contributed to a small increase in fatalities due to the more frequent cold extremes in Stockholm, Sweden (Åström et al. 2013). It is very likely that the Arctic sea ice cover will continue to shrink and thin during the twenty-first century with continued global warming (IPCC 2013), therefore, increased SAT variability over East Asia is expected. Instead of decreasing the cold-season mortality rate over East Asia, the Arctic warming associated with AA may increase it, and the cold extreme–related risks for human health, agriculture, and economic development may still exist in this region despite ongoing global and Arctic warming.

b. Discussion

In this study, we conclude that the circulation effects of AA during the cold season in Eurasia are dominated by increased blocking events over the Urals and an amplified SH, resulting in more cold extremes over East Asia. Together with the more frequent and warmer warm extremes due to the thermodynamic effect of global warming, the AA has significantly contributed to the increased cold-season SAT variability over East Asia in the era of AA. It should be noted that, in addition to being significantly influenced by global, in particular Arctic warming, there are energetic internal fluctuations in the atmospheric circulation in winter over Eurasia (Park et al. 2011; Cheung et al. 2012; Cohen et al. 2014; Wallace et al. 2014; Overland et al. 2016; Cohen 2016). It has been demonstrated that the AO, the most representative atmospheric variation for internal dynamics of the Northern Hemisphere circulation during cold seasons, is closely connected to the behavior of the East Asian winter monsoon (Park et al. 2011; Cheung et al. 2012; Ding et al. 2014). Although no clear evidence of the influence of the AO on the East Asian SAT variability during cold seasons is detected, the AO has a significant impact on cold extremes over East Asia, with the correlation between the AO index and East Asian cold extremes being -0.46 and -0.45 for time series with and without trends, respectively, and significant at the 0.01 level. Park et al. (2011) also reported that the cold surges over East Asia during negative AO periods are more frequent and stronger in terms of both magnitude and duration than those during positive AO periods. Thus, how to quantify the relative contribution of Arctic warming and natural internal variability, such as the AO, to the increase of the cold extremes over East Asia in the era of AA is a very interesting scientific question.

In contrast to the increasing trend of the daily SAT variability during the cold season in the rest of China, a significantly decreasing trend has appeared over the Tibetan Plateau in the era of AA. A similar phenomenon was found in the winter mean SAT. For instance, during the cold period (1960/61–1985/86) and hiatus period (2006/07–2012/13), a warming trend was observed over the Tibetan Plateau, while a cooling trend was found in other parts of China, and during the warm period (1986/87–2005/06); however, the former warming and cooling trends become opposite between the Tibetan Plateau and the rest of China (Ding et al. 2014; Duan and Xiao 2015). Duan and Xiao (2015) suggested that cloud–radiation feedbacks may play an important role in modulating the recent warming trend over the Tibetan Plateau. It is an open question whether the

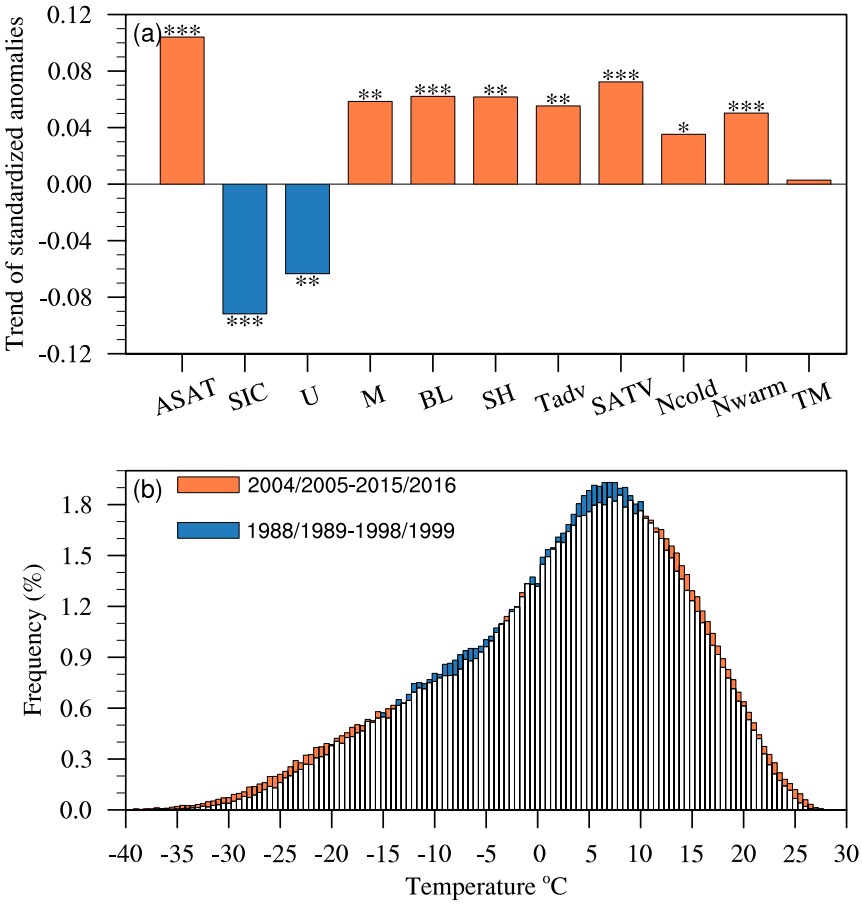

FIG. 10. (a) Linear trends of the standardized cold-season mean Arctic SATs (ASAT) averaged over the region of 60°–90°N, 0°–360°E, sea ice concentrations (SIC) averaged over the Barents–Kara Sea (65°–85°N, 30°–90°E), zonal winds at 500 hPa (U) averaged over Asia (50°–70°N, 70°–120°E), meandering index (M) defined over the Eurasian sector, incidence of blockings (BL) averaged over the Ural region (50°–80°N, 45°–90 °E), SH intensity (defined as the area-mean SLP of 40°–65°N, 70°–120°E), East Asia (20°–52°N, 103°–125°E) averaged cold temperature advection (Tadv) at 850 hPa, variability of the daily mean SAT (SATV), extremely cold days (Ncold), extremely warm days (Nwarm), and cold-season mean temperatures (TM) during 1988/89–2015/16. The 90%, 95%, and 99% significances are labeled by *, **, and ***, respectively. (b) Histogram of the cold-season daily temperatures averaged over eastern China during the period of 1988/89–1998/99 (blue bars) with Arctic SAT anomalies mostly negative and the other period of 2004/05–2015/16 (orange bars) with Arctic SAT anomalies mostly positive. White shows the overlap distribution. East Asian SATs are taken from NMIC; other variables are taken from the ERA-Interim reanalysis.

observed difference of the trend in the cold-season daily SAT variability over the Tibetan Plateau and other areas of China is due to cloud–radiation feedback or other factors. The reasons for the above difference merit further investigations.

In this study, inspired by the strong weather whiplash phenomenon over East Asia during the cold season of 2015/16, we analyzed the change of East Asian SAT variability in the era of AA and found a significantly increasing trend of weather whiplash that is strongly associated with the AA effect. However, the direct attribution of the impact of global, especially Arctic, warming on the cold extremes during the winter of 2015/16 could not be performed with the observationally based framework used for this study. Motivated by the understanding of the mechanism of AA influence on cold-season SAT variability over East Asia revealed by the present study, future work should use modeling frameworks to attribute these record-breaking cold extremes and determine how much the probability of cold extremes over East Asia similar to or more serious than those of 2015/16 is increased by anthropogenic climate change.

Acknowledgments. This study was jointly supported by the National Natural Science Foundation of China (41705052, 41475057, 91637312, and 41775052), the Special Funds for Climate Change (CCSF201830), and the Basic Scientific Research and Operation Foundation of CAMS (2015Z001 and 2017R001).

REFERENCES

Åström, D. O., B. Forsberg, K. L. Ebi, and J. Rocklöv, 2013: Attributing mortality from extreme temperatures to climate change in Stockholm, Sweden. *Nat. Climate Change*, **3**, 1050–1054, https://doi.org/10.1038/nclimate2022.

Barnes, E. A., E. Dunn-Sigouin, G. Masato, and T. Woollings, 2014: Exploring recent trends in Northern Hemisphere blocking. *Geophys. Res. Lett.*, **41**, 638–644, https://doi.org/10.1002/2013GL058745.

Cheung, H. N., W. Zhou, H. Y. Mok, and M. C. Wu, 2012: Relationship between Ural–Siberian blocking and the East Asian winter monsoon in relation to the Arctic Oscillation and the El Niño–Southern Oscillation. *J. Climate*, **25**, 4242–4257, https://doi.org/10.1175/JCLI-D-11-00225.1.

Christidis, N., G. S. Jones, and P. A. Stott, 2015: Dramatically increasing chance of extremely hot summers since the 2003 European heatwave. *Nat. Climate Change*, **5**, 46–50, https://doi.org/10.1038/nclimate2468.

CMA, 2016: Global major weather and climate event in January 2016 (in Chinese). China Meteorological News Press, http://www.cma.gov.cn/2011xwzx/2011xqxxw/2011xqxyw/201602/t20160210_303989.html.

——, 2017: China Climate Bulletin for 2016 (in Chinese). China Meteorological Administration, 35 pp., http://www.cma.gov.cn/root7/auto13139/.

Cohen, J., 2016: An observational analysis: Tropical relative to Arctic influence on midlatitude weather in the era of Arctic amplification. *Geophys. Res. Lett.*, **43**, 5287–5294, https://doi.org/10.1002/2016GL069102.

——, J. C. Furtado, M. A. Barlow, V. A. Alexeev, and J. E. Cherry, 2012: Arctic warming, increasing snow cover and widespread boreal winter cooling. *Environ. Res. Lett.*, **7**, 014007, https://doi.org/10.1088/1748-9326/7/1/014007.

——, and Coauthors, 2014: Recent Arctic amplification and extreme mid-latitude weather. *Nat. Geosci.*, **7**, 627–637, https://doi.org/10.1038/ngeo2234.

Dee, D. P., and Coauthors, 2011: The ERA-Interim reanalysis: Configuration and performance of the data assimilation system. *Quart. J. Roy. Meteor. Soc.*, **137**, 553–597, https://doi.org/10.1002/qj.828.

Di Capua, G., and D. Coumou, 2016: Changes in meandering of the Northern Hemisphere circulation. *Environ. Res. Lett.*, **11**, 094028, https://doi.org/10.1088/1748-9326/11/9/094028.

Ding, Y., and Coauthors, 2014: Interdecadal variability of the East Asian winter monsoon and its possible links to global climate change. *J. Meteor. Res.*, **28**, 693–713, https://doi.org/10.1007/s13351-014-4046-y.

Duan, A., and Z. Xiao, 2015: Does the climate warming hiatus exist over the Tibetan Plateau?. *Sci. Rep.*, **5**, 13711, https://doi.org/10.1038/srep13711.

Fischer, E. M., and R. Knutti, 2015: Anthropogenic contribution to global occurrence of heavy-precipitation and high-temperature extremes. *Nat. Climate Change*, **5**, 560–564, https://doi.org/10.1038/nclimate2617.

Francis, J. A., and S. J. Vavrus, 2012: Evidence linking Arctic amplification to extreme weather in mid-latitudes. *Geophys. Res. Lett.*, **39**, L06801, https://doi.org/10.1029/2012GL051000.

Hansen, J., R. Ruedy, M. Sato, and K. Lo, 2010: Global surface temperature change. *Rev. Geophys.*, **48**, RG4004, https://doi.org/10.1029/2010RG000345.

Honda, M., J. Inoue, and S. Yamane, 2009: Influence of low Arctic sea-ice minima on anomalously cold Eurasian winters. *Geophys. Res. Lett.*, **36**, L08707, https://doi.org/10.1029/2008GL037079.

Horton, D. E., N. C. Johnson, D. Singh, D. L. Swain, B. Rajaratnam, and N. S. Diffenbaugh, 2015: Contribution of changes in atmospheric circulation patterns to extreme temperature trends. *Nature*, **522**, 465–469, https://doi.org/10.1038/nature14550.

Hoskins, B. J., and T. Ambrizzi, 1993: Rossby wave propagation on a realistic longitudinally varying flow. *J. Atmos. Sci.*, **50**, 1661–1671, https://doi.org/10.1175/1520-0469(1993)050<1661:RWPOAR>2.0.CO;2.

Inoue, J., M. E. Hori, and K. Takaya, 2012: The role of Barents Sea ice in the wintertime cyclone track and emergence of a warm-Arctic cold-Siberian anomaly. *J. Climate*, **25**, 2561–2568, https://doi.org/10.1175/JCLI-D-11-00449.1.

IPCC, 2012: Summary for policymakers. *Managing the Risks of Extreme Events and Disasters to Advance Climate Change Adaptation*, C. B. Field et al., Eds., Cambridge University Press, 3–21.

——, 2013: Summary for policymakers. *Climate Change 2013: The Physical Science Basis*, T. F. Stocker et al., Eds., Cambridge University Press, 1–29.

Kug, J.-S., J.-H. Jeong, Y.-S. Jang, B.-M. Kim, C. K. Folland, S.-K. Min, and S.-W. Son, 2015: Two distinct influences of Arctic warming on cold winters over North America and East Asia. *Nat. Geosci.*, **8**, 759–762, https://doi.org/10.1038/ngeo2517.

Liu, J., J. A. Curry, H. Wang, M. Song, and R. M. Horton, 2012: Impact of declining Arctic sea ice on winter snowfall. *Proc. Natl. Acad. Sci. USA*, **109**, 4074–4079, https://doi.org/10.1073/pnas.1114910109.

Liu, X., and Z. Ren, 2005: Progress in quality control of surface meteorological data. *Mater. Sci. Technol.*, **33**, 199–203.

Luo, D., Y. Yao, A. Dai, I. Simmonds, and L. Zhong, 2017: Increased quasi stationarity and persistence of winter Ural blocking and Eurasian extreme cold events in response to Arctic warming. Part II: A theoretical explanation. *J. Climate*, **30**, 3569–3587, https://doi.org/10.1175/JCLI-D-16-0262.1.

Mori, M., M. Watanabe, H. Shiogama, J. Inoue, and M. Kimoto, 2014: Robust Arctic sea-ice influence to frequent Eurasian cold winters in past decades. *Nat. Geosci.*, **7**, 869–873, https://doi.org/10.1038/ngeo2277.

Nakamura, H., K. Nishii, L. Wang, Y. J. Orsolini, and K. Takaya, 2016: Cold-air outbreaks over East Asia associated with blocking highs: Mechanisms and their interaction with the polar stratosphere. *Dynamics and Predictability of Large-Scale High-Impact Weather and Climate Events*, J. Li et al., Eds., Cambridge University Press, 225–235.

Orsolini, Y. J., R. Senan, R. E. Benestad, and A. Melsom, 2012: Autumn atmospheric response to the 2007 low Arctic sea ice extent in coupled ocean–atmosphere hindcasts. *Climate Dyn.*, **38**, 2437–2448, https://doi.org/10.1007/s00382-011-1169-z.

——, ——, G. Balsamo, F. J. Doblas-Reyes, F. Vitart, A. Weisheimer, A. Carrasco, and R. Benestad, 2013: Impact of snow initialization on sub-seasonal forecasts. *Climate Dyn.*, **41**, 1969–1982, https://doi.org/10.1007/s00382-013-1782-0.

Overland, J. E., and Coauthors, 2016: Nonlinear response of mid-latitude weather to the changing Arctic. *Nat. Climate Change*, **6**, 992–999, https://doi.org/10.1038/nclimate3121.

Park, T.-W., C.-H. Ho, and S. Yang, 2011: Relationship between the Arctic Oscillation and cold surges over East Asia. *J. Climate*, **24**, 68–83, https://doi.org/10.1175/2010JCLI3529.1.

——, ——, and Y. Deng, 2014: A synoptic and dynamical characterization of wave-train and blocking cold surge over East Asia. *Climate Dyn.*, **43**, 753–770, https://doi.org/10.1007/s00382-013-1817-6.

Rhines, A., K. A. McKinnon, M. P. Tingley, and P. Huybers, 2017: Seasonally resolved distributional trends of North American temperatures show contraction of winter variability. *J. Climate*, **30**, 1139–1157, https://doi.org/10.1175/JCLI-D-16-0363.1.

Screen, J. A., 2014: Arctic amplification decreases temperature variance in northern mid- to high-latitudes. *Nat. Climate Change*, **4**, 577–582, https://doi.org/10.1038/nclimate2268.

——, 2017: The missing northern European winter cooling response to Arctic sea ice loss. *Nat. Commun.*, **8**, 14603, https://doi.org/10.1038/ncomms14603.

——, C. Deser, and L. Sun, 2015: Reduced risk of North American cold extremes due to continued Arctic sea ice loss. *Bull. Amer. Meteor. Soc.*, **96**, 1489–1503, https://doi.org/10.1175/BAMS-D-14-00185.1.

Shepherd, T. G., 2016: Effects of a warming Arctic. *Science*, **353**, 989–990, https://doi.org/10.1126/science.aag2349.

Sun, L., J. Perlwitz, and M. Hoerling, 2016: What caused the recent "warm Arctic, cold continents" trend pattern in winter temperatures? *Geophys. Res. Lett.*, **43**, 5345–5352, https://doi.org/10.1002/2016GL069024.

Sun, Y., X. Zhang, F. W. Zwiers, L. Song, H. Wan, T. Hu, H. Yin, and G. Ren, 2014: Rapid increase in the risk of extreme summer heat in eastern China. *Nat. Climate Change*, **4**, 1082–1085, https://doi.org/10.1038/nclimate2410.

Takaya, K., and H. Nakamura, 2001: A formulation of a phase-independent wave-activity flux for stationary and migratory quasigeostrophic eddies on a zonally varying basic flow. *J. Atmos. Sci.*, **58**, 608–627, https://doi.org/10.1175/1520-0469(2001)058<0608:AFOAPI>2.0.CO;2.

——, and ——, 2005: Mechanisms of intraseasonal amplification of the cold Siberian high. *J. Atmos. Sci.*, **62**, 4423–4440, https://doi.org/10.1175/JAS3629.1.

Tang, Q., X. Zhang, X. Yang, and J. A. Francis, 2013: Cold winter extremes in northern continents linked to Arctic sea ice loss. *Environ. Res. Lett.*, **8**, 014036, https://doi.org/10.1088/1748-9326/8/1/014036.

Van Oldenborgh, G. J., R. Haarsma, H. De Vries, and M. R. Allen, 2015: Cold extremes in North America vs. mild weather in Europe: The winter of 2013–14 in the context of a warming world. *Bull. Amer. Meteor. Soc.*, **96**, 707–714, https://doi.org/10.1175/BAMS-D-14-00036.1.

Wallace, J. M., I. M. Held, D. W. J. Thompson, K. E. Trenberth, and J. E. Walsh, 2014: Global warming and winter weather. *Science*, **343**, 729–730, https://doi.org/10.1126/science.343.6172.729.

Wang, L., W. Chen, W. Zhou, J. C. L. Chan, D. Barriopedro, and R. Huang, 2010: Effect of the climate shift around mid 1970s on the relationship between wintertime Ural blocking circulation and East Asian climate. *Int. J. Climatol.*, **30**, 153–158, https://doi.org/10.1002/joc.1876.

Yang, Z., W. Huang, B. Wang, R. Chen, J. S. Wright, and W. Ma, 2018: Possible mechanisms for four regimes associated with cold events over East Asia. *Climate Dyn.*, https://doi.org/10.1007/s00382-017-3905-5, in press.

Yao, Y., D. Luo, A. Dai, and I. Simmonds, 2017: Increased quasi stationarity and persistence of winter Ural blocking and Eurasian extreme cold events in response to Arctic warming. Part I: Insights from observational analyses. *J. Climate*, **30**, 3549–3568, https://doi.org/10.1175/JCLI-D-16-0261.1.

Zhai, P., and Coauthors, 2016: The strong El Niño in 2015/16 and its dominant impacts on global and China's climate. *J. Meteor. Res.*, **30**, 283–297, https://doi.org/10.1007/s13351-016-6101-3.

Zhang, X., C. Lu, and Z. Guan, 2012: Weakened cyclones, intensified anticyclones and recent extreme cold winter weather events in Eurasia. *Environ. Res. Lett.*, **7**, 044044, https://doi.org/10.1088/1748-9326/7/4/044044.

Zhang, Y., K. R. Sperber, and J. S. Boyle, 1997: Climatology and interannual variation of the East Asian winter monsoon: Results from the 1979–95 NCEP/NCAR reanalysis. *Mon. Wea. Rev.*, **125**, 2605–2619, https://doi.org/10.1175/1520-0493(1997)125<2605:CAIVOT>2.0.CO;2.